9894–9904 *Nucleic Acids Research, 2023, Vol. 51, No. 18* *Published online 31 August 2023*
https://doi.org/10.1093/nar/gkad715

Unidirectional *trans*-cleaving behavior of CRISPR-Cas12a unlocks for an ultrasensitive assay using hybrid DNA reporters containing a 3′ toehold

Noor Mohammad[1,2], Logan Talton[1], Zach Hetzler[1], Megha Gongireddy[1] and Qingshan Wei[1,*]

[1]Department of Chemical and Biomolecular Engineering, North Carolina State University, Raleigh, NC 27695, USA and [2]Department of Chemical Engineering, Bangladesh University of Engineering and Technology, Dhaka 1000, Bangladesh

Received June 01, 2023; Revised August 04, 2023; Editorial Decision August 07, 2023; Accepted August 19, 2023

ABSTRACT

CRISPR-Cas12a can induce nonspecific *trans*-cleavage of dsDNA substrate, including long and stable λ DNA. However, the mechanism behind this is still largely undetermined. In this study, we observed that while *trans*-activated Cas12a didn't cleave blunt-end dsDNA within a short reaction time, it could degrade dsDNA reporters with a short overhang. More interestingly, we discovered that the location of the overhang also affected the susceptibility of dsDNA substrate to *trans*-activated Cas12a. Cas12a *trans*-cleaved 3′ overhang dsDNA substrates at least 3 times faster than 5′ overhang substrates. We attributed this unique preference of overhang location to the directional *trans*-cleavage behavior of Cas12a, which may be governed by RuvC and Nuc domains. Utilizing this new finding, we designed a new hybrid DNA reporter as nonoptical substrate for the CRISPR-Cas12a detection platform, which sensitively detected ssDNA targets at sub picomolar level. This study not only unfolded new insight into the *trans*-cleavage behavior of Cas12a but also demonstrated a sensitive CRISPR-Cas12a assay by using a hybrid dsDNA reporter molecule.

GRAPHICAL ABSTRACT

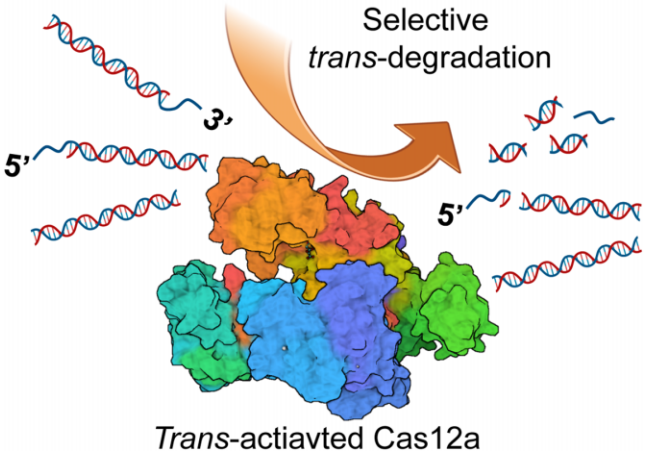

INTRODUCTION

CRISPR (short for Clustered Regularly Interspaced Short Palindromic Repeats) was discovered as an adaptive immune system in bacteria and archaea by protecting them from foreign invasive species such as bacteriophages and plasmids (1–3). CRISPR and its associated protein (aka. CRISPR-Cas) was initially applied as a genome editing tool (4–7) and now has evolved as a promising diagnostic platform (8–11). The CRISPR-Cas system has been an emerging alternative to conventional polymerase chain reaction (PCR) or DNA sequencing for nucleic acid detection. CRISPR-based diagnostics (CRISPR-Dx) is rapid, sensitive, specific, cost-effective, and well-suited for point-of-care (POC) testing (12).

Among numerous CRISPR-Cas systems, CRISPR-Cas12a (aka. Cpf1) and CRISPR-Cas13a (aka. C2c2) are most widely explored for rapid and accurate nucleic acid diagnosis (8,9). For instance, CRISPR-Cas13-based

*To whom correspondence should be addressed. Tel: +1 919 515 3154; Email: qwei3@ncsu.edu

Specific High-Sensitivity Enzymatic Reporter UnLOCKing (SHERLOCK) (9) and CRISPR-Cas12-based DNA Endonuclease Targeted CRISPR Trans Reporter (DETECTR) (8) have been developed as promising diagnostic platforms for detecting RNA and DNA, respectively. Since CRISPR assay is an isothermal process that requires no thermocycling or any other complex laboratory setup (13), the CRISPR-Dx platform is well positioned for POC disease diagnosis (14). Till now, CRISPR-Dx has matured significantly and been demonstrated in various detection formats, including optical (8,9,15–22), nonoptical (23,24), preamplification-free (21,22,25,26), nucleic acid extraction-free (18,27–29), lateral flow assays, (19,30–32), digital CRISPR (33–36) and multiplex detection format (15,37–39). The CRISPR-Cas system has found broad applications in disease diagnosis (8,16,31,40–42) and mutation detection (37,43). The central concept of Cas12a or Cas13a-based diagnostics is all based on a simple principle, which is the *trans*-cleavage of single-stranded (ss) oligonucleotide substrates (also called reporters) upon target recognition.

While it is widely established that CRISPR-Cas12a shows no or minimal *trans*-cleavage towards double-stranded (ds) DNA substrate (8), a few early CRISPR-Dx studies showed that certain Cas12a variants (i.e. LbCas12a, BoCas12a and Lb4Cas12a) had a notable *trans*-degradation activity on dsDNA substrates (44). Recently, several groups utilized the dsDNA *trans*-cleavage activity of LbCas12a to develop biosensors (12,45,46). In most cases, the *trans*-cleavage of dsDNA was mainly attributed to the instability of dsDNA reporters due to their short length (typically $< \sim$30 bp) (45,46) or the presence of ssDNA looped structures on the dsDNA backbone (12). The effect of salt concentration (45,47) and magnesium ion (Mg^{2+}) (47) on dsDNA degradation has also been studied. However, the exact mechanism behind Cas12a-based *trans*-degradation of dsDNA has not been fully understood yet.

Here, we performed a new investigation into the nonspecific dsDNA *trans*-cleavage behavior of Cas12a and found an interesting 3′ overhang switch, which can turn inactive blunt-end dsDNA substrates into *trans*-degradable reporter molecules for Cas12a. We compared the *trans*-cleavage activity of Cas12a using various dsDNA substrates with 3′ or 5′ overhangs and found that Cas12a preferentially *trans*-degraded 3′ overhang dsDNA over 5′ overhang dsDNA. We hypothesize that the overhang preference is related to the directional enzymatic behavior of Cas12a (3′ → 5′), which may be controlled by the RuvC and Nuc domains. These findings bring in a new design for more cost-effective (nonoptical) reporter molecules, which is based on a hybrid structure: a dsDNA backbone with a short ssDNA overhang at 3′ end. Utilizing these hybrid reporters, we constructed a sensitive CRISPR-Cas12a diagnostic assay that can detect ssDNA targets down to sub picomolar level by combining naked-eye detection and gel electrophoresis without preamplification. Finally, we demonstrated the use of the hybrid reporter CRISPR-Cas12a assay for the detection of adeno-associated viruses (AAV) and human papillomavirus 16 (HPV 16) as model targets. To the best of our knowledge, this is the first report describing the unidirectional *trans*-cleaving behavior of Cas12a and significant role of ss overhang on *trans*-degrading dsDNA substrate.

MATERIALS AND METHODS

Chemicals and apparatus

LbaCas12a, gRNAs, synthetic targets and all oligonucleotides were purchased from Integrated DNA Technologies (IDT, Coralville, IA, USA). NEB2.1 was purchased from New England Biolabs (MA, USA). Ultrapure water (18.3 MΩ cm) was produced by the Milli-Q system (Millipore, Inc., USA) and used throughout the experiments. The sequences of oligonucleotides and gRNA molecules are listed in Supplementary Table S1.

CRISPR-LbaCas12a assays

All DNA and RNA oligos were stored in 10 mM Tris–HCl buffer (pH 7.5) at 10 μM concentrations in a –20°C refrigerator and pre-warmed at 37°C for ∼30 min before mixing. For the CRISPR assay, analyte solutions with different concentrations of synthetic ssDNA were added into the CRISPR reaction reagents, consisting of 40 nM LbaCas12a, 20 nM gRNA, 400–800 nM dsDNA as reporter (nonspecific substrate).(36) The reaction was done in NEB2.1 buffer (50 mM NaCl, 10 mM Tris–HCl, 10 mM $MgCl_2$, 100 μg/ml BSA maintaining pH = 7.9 @ 25°C). The total reaction volume was 80–120 μl.

Gel electrophoresis

Gel electrophoresis was performed as the nonfluorescent reporting system (12). 2–4% agarose gels were prepared using 1 × TBE buffer (89 mM Tris, 89 mM borate acid, 2 mM EDTA, pH 8.3). 5 μl of different reaction products with loading dye (5:1, v/v) were added to each well. Electrophoresis was done at 90–100 V for 60–70 min in the same buffer at room temperature. Finally, the agarose gels were scanned and recorded by the E-Gel Imager system (Invitrogen, USA).

Gel image analysis

ImageJ software was used to analyze the gels. First, background was removed from the gel image to exclude noise. The longitudinal intensity of each lane was averaged across the width of each lane and plotted along the longitudinal axis. Normalized intensities (peak intensity for each concentration divided by the peak intensity of the negative control) were plotted against the concentration of the ssDNA target for different types of reporter molecules (i.e. Ra-3′ & Ra-5′).

Quantitative cleavage of dsDNA

Qubit Flex fluorometer (Invitrogen, Thermofisher scientific)was used for measuring the extent of dsDNA present in the reaction mixture at different time points. At a certain time, 5 μl of reaction mixture was added to 195 μl dsDNA working solution (Catalog#Q32854) containing an intercalating dye that specifically binds to the dsDNA backbone. After a gentle vortex, the mixture was incubated for 2 min at room temperature, wrapped in aluminum foil. Then, the

Qubit Flex fluorometer was used to measure the concentration of dsDNA in the sample. We repeated this procedure for each sample taken at different time points to get the quantitative degradation of dsDNA reporter with *trans*-activated Cas12a.

Reaction kinetics study

To evaluate the reaction kinetics for various reporters, we generated Michaelis-Menten (MM) plot. For this purpose, 40 nM LbCas12a, 20 nM rRNA, and 15 nM ssDNA target were mixed to run CRISPR assay. Pre-prepared dsDNA reporters of different concentrations (40 nM-600 nM) were added to the reaction mixture, and the reaction was run at 37°C for 2 h with Qubit reading at time intervals of 10 min/20 min/30 min. The initial velocity (V_0) was calculated by fitting the data to a linear regression. Then, V_0 was plotted against the substrate (dsDNA reporter) concentration to determine the MM constants (GraphPad Software) according to the following equation: (8)

$$Y = (V_{max} \times X) / (K_m + X)$$

where X is the substrate concentration and Y is the enzymatic velocity. The turnover number (k_{cat}) was determined by the following equation:

$$k_{cat} = V_{max}/E_t$$

where $E_t = 15$ nM.

RESULTS AND DISCUSSION

CRISPR-cas12a-based *trans*-degradation of dsDNA with an overhang

Canonical CRISPR-Dx studies suggest that CRISPR-Cas12a *trans*-cleaves ssDNA substrate only (8), and a myriad number of biosensors have been developed based on CRISPR-Cas12a and ssDNA reporters (8,10,14,23). Cas12a typically does not *trans*-cleave dsDNA because the RuvC catalytic pocket cannot accommodate dsDNA (48). However, we previously observed very long ds λ DNA could be effectively *trans*-degraded by Cas12a (12), which is quite contradictory to the conventional knowledge. In that research, we hypothesized the ss loop structures along the λ DNA backbone might play a significant role in promoting λ DNA's susceptibility to Cas12a (12). We verified the previous hypothesis by introducing ss loop structures into short synthetic dsDNA reporters and did observe significantly enhanced *trans*-cleavage activities of loop-containing dsDNA reporters compared to blunt-end controls. Here, we investigated if a ssDNA overhang could act as the initiation site (where the RuvC cavity could cut) for *trans*-activated Cas12a, similar to the plausible role of ss loop structures in λ DNA. If it is true, it would further confirm our previous observations on λ DNA and prove the importance of ss sequences in *trans*-cleaving dsDNA substrates mediated by Cas12a.

To test this idea, we performed a CRISPR-Cas12a assay based on LbCas12a effector with two different reporters: one is 60-bp blunt-end dsDNA (named Ra), and the other has the same sense strand but a few nts (e.g. 12 nts) shorter in the antisense strand to make a 3′ toehold (named Ra-3′, Figure 1A). We observed that in the presence of 125 nM ssDNA target concentration, Cas12a did not cleave 60-bp blunt-end dsDNA reporter (Ra) after 60 min of reaction (Figure 1A, lane 2), which is consistent with the conventional knowledge that CRISPR-Cas12a does not show nonspecific *trans*-cleavage on dsDNA substrates (8). For the second reporter (Ra-3′), we observed a complete degradation of reporters at 125 nM target concentration (Figure 1A, lane 4). We confirmed similar results with repeated experiments performed at 25 and 125 nM concentrations using the same pair of reporter molecules (Supplementary Figure S1a). In addition, we designed a new set of reporters (Rb and Rb-3′) with a similar length (60 bp) and structure (blunt-end vs. overhang) but different sequences and physical properties (i.e. higher GC content, etc.). The detailed parameters of Ra and Rb reporters are listed in Supplementary Table S2. With this new set of reporter molecules (Rb and Rb-3′), the gel results again showed that the presence of a 3′ overhang on dsDNA could help degrade the dsDNA substrate (Rb-3′) with target-activated Cas12a (Supplementary Figure S1b). On the other end, blunt-end dsDNA substrate (Rb) was mostly kept intact under similar reaction conditions.

Next, we checked the minimum length of overhang required to turn on the *trans*-cleavage activity of dsDNA substrates. We performed CRISPR reaction with the dsDNA reporters containing 0, 4, 8 and 12-nt overhang at the 3′ end. Even though 4-nt overhang showed *trans*-cleavage at high target concentration (250 nM), we observed that overhang length shorter than 8 nts showed much less *trans*-cleavage activities at 25 nM target concentration (Figure 1B). This suggests that when *cis*-activated Cas12a searches for ssDNA, it needs minimally ∼8-nt long oligonucleotide sequence to grab on. This could also explain why the shorter F-Q reporter (5 nts) showed lower *trans*-cleavage activity compared to the longer ones (10 or 15 nts) in the previous studies (49). Besides, we explored if there was a maximum overhang length, beyond which Cas12a might not efficiently degrade the whole ds backbone. We tested dsDNA reporters with 22, 32, and 52-nt overhangs. The results were identical to 12-nt overhang dsDNA reporter, suggesting that any overhang length above 8-nt can act as the switch for initiating *trans*-cleavage of whole dsDNA (Supplementary Figure S2). Further increasing the overhang length will equivalently turn dsDNA reporters into ssDNA reporters, which is known to be susceptible to the *trans*-cleavage of Cas12a.

Previously, a few studies showed that certain dsDNA could be *trans*-degraded. Researchers generally attributed the degradation of short dsDNA reporters to the weak hybridization between sense and antisense strands (45,46). For long dsDNA (e.g. λ DNA), we attributed the *trans*-cleaving behavior of λ DNA reporters to the presence of ssDNA loop structures along the dsDNA backbone (12). Additionally, research also showed that *cis*-activated Cas12a could also nick, relax, and slowly *trans*-degrade supercoiled dsDNA (50). However, to the best of our knowledge, this is the first experimental evidence showing that adding a ss overhang to blunt-end dsDNA substrate could fundamentally change its *trans*-cleavage property.

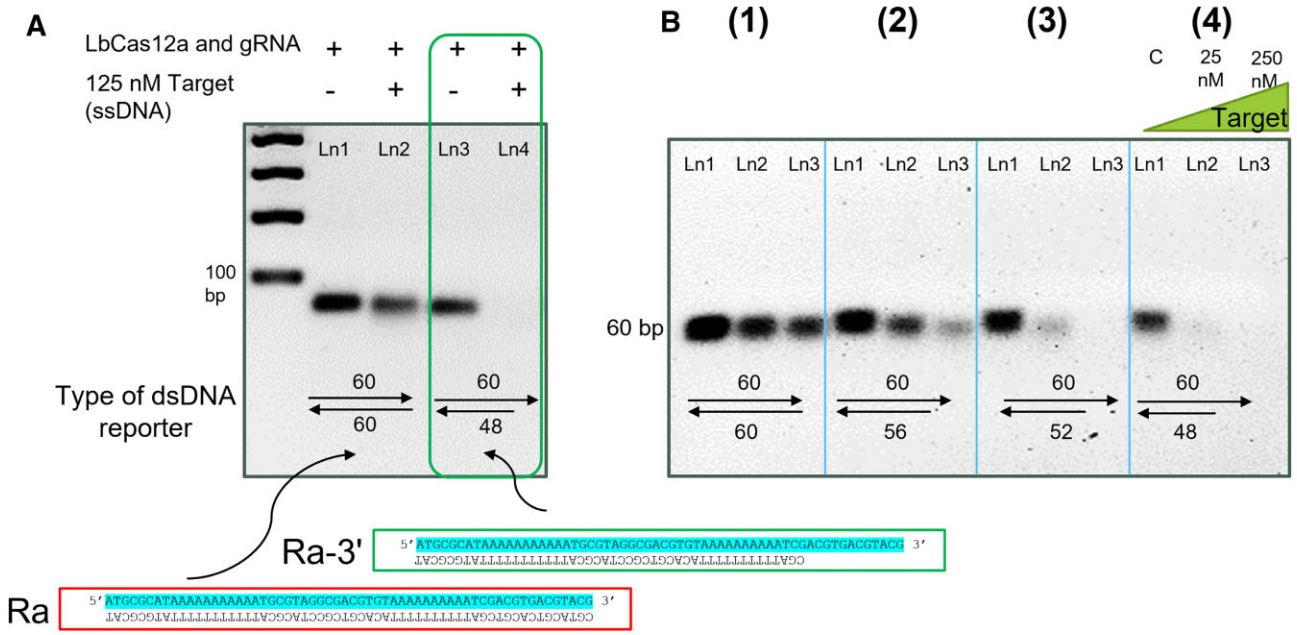

Figure 1. Gel electrophoresis (2% agarose gel and 1 × TBE buffer) results demonstrate the nonspecific degradation of dsDNA substrates with overhangs by *trans*-activated Cas12a. (**A**) CRISPR-Cas12a reaction using dsDNA reporters w/ and w/o overhangs. Ra is a 60-bp blunt-end dsDNA reporter; Ra-3′ is derived from Ra by removing 12 nts from the antisense strand to make a 3′ toehold. Cyan shade in Ra and Ra-3′ indicates that the sense strand sequences are exactly the same. (**B**) Effect of overhang length on Cas12a *trans*-cleavage. In each panel of (B), Ln1: negative control (no target); Ln2 and Ln3: experimental lanes with target concentrations of 25 and 250 nM, respectively. Abbreviations: gRNA, guide RNA; ssDNA, single-stranded DNA; dsDNA, double-stranded DNA; nM, nanomolar; bp, base pair; Ln, lane; c, negative control; TBE, Tris-borate EDTA; nt, nucleotide.

Overhang-mediated unidirectional *trans*-cleavage

More interestingly, we observed the location of overhang is also critical in activating dsDNA substrates for Cas12a-based *trans*-cleavage. We explored Cas12a-induced *trans*-degradation using dsDNA reporters with both 3′ and 5′ overhangs. These reporters contain the same sense strand, or same overhang sequence, or same ds backbone sequence. We also characterized the reaction kinetics for 3′ and 5′ overhang dsDNA reporters containing the same ds backbone with same overhang sequence.

Trans-degradation of 3′ and 5′ overhang dsDNA reporter containing the same sense strand

We first used the same sense stand (60 nt) and constructed two different overhangs: 3′ and 5′ overhangs by removing 12 nts from the antisense strand (Ra-3′ and Ra-5′, Figure 2A). We then performed CRISPR-Cas12a assay using above two reporters (Ra-3′ and Ra-5′) as the nonspecific substrates. Initially, we expected a similar *trans*-degradation result for both reporters since both have the same length, same sense strand, and same length of overhang. Surprisingly, we observed remarkably different *trans*-cleaving activities of the two reporters. For the 3′ overhang reporter (Ra-3′, which was also used in Figure 1A, lanes 3 and 4), we observed complete degradation with target concentrations above 25 nM (Figure 2A). However, for the 5′ overhung reporter (Ra-5′), no complete degradation was observed. Instead, we noticed a slight downshift of the gel bands, indicating the trimming of ss overhangs instead of degrading the dsDNA backbones. We also performed the assay using two more sets of reporters (Rb and Rc) with different sense strand sequences (Supplementary Table S1). In each case, we observed that reporters with 3′ overhang significantly outperformed (in terms of getting *trans*-degraded) 5′ overhang dsDNA, regardless of actual sequences of sense strands (Supplementary Figures S3b and S3c).

To quantify the extent of *trans*-cleaving, the intensities of each lane were averaged across the width of the lane and plotted against the long axis following a similar process as described in the previous report (12). Figure 2B shows that the intensity peak of Ra-3′ reporter vanished at 250 nM target concentration. In contrast, for Ra-5′ reporter, the intensity of bands remained prominent over all the target concentrations experimented. However, the peak position shifted slightly rightward for higher target concentrations due to the trimming of the overhang, which reduced the length of the Ra-5′ reporter slightly. The normalized lane intensity values were plotted in bar chart against different target concentrations (Figure 2C). We observed that normalized lane intensities for Ra-3′ reporter (purple bars) were much lower than that for Ra-5′ reporter (orange bars) at 25 and 250 nM target concentrations, suggesting different *trans*-cleavage activities.

We performed additional control experiments to confirm that the observed overhang preference is not dependent on overhang density or specific configuration. For that, we kept the sense stand the same and shifted the antisense strand to the right to create double 5′ overhangs on both ends (named Ra-5′5’ reporter, Supplementary Figure S3a, middle panel). We performed CRISPR-Cas12a reaction with all three different reporters (Ra-5′, Ra-3′, and Ra-5′5’, Supplementary Figure S3a). Our results showed that Ra-5′5’ yielded a

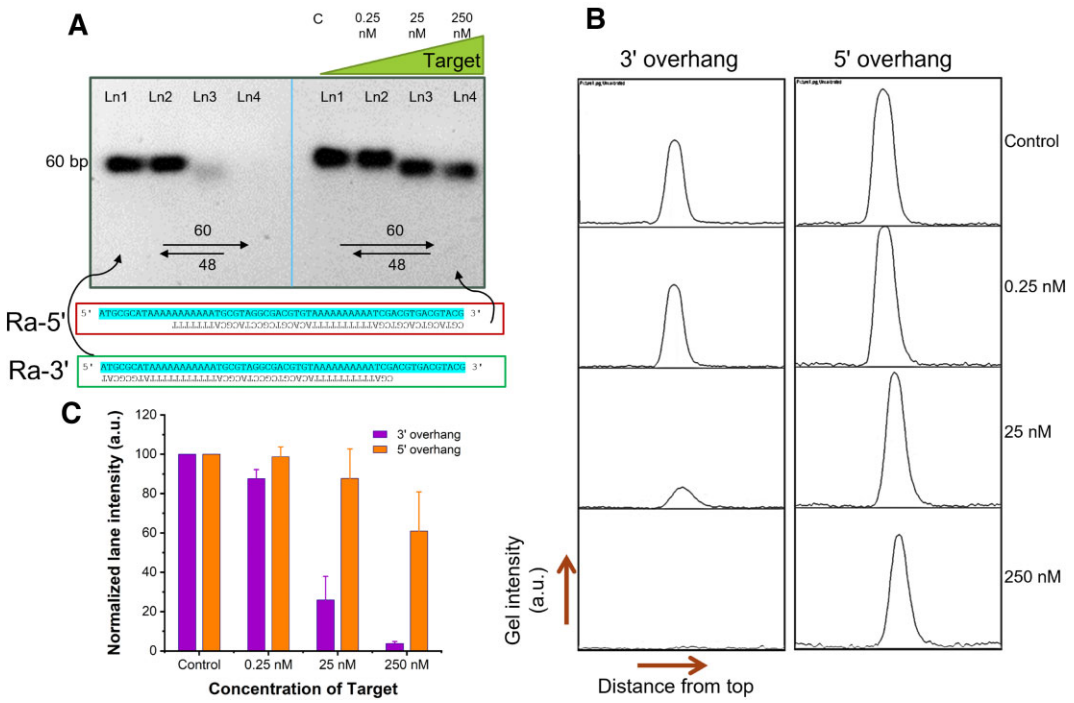

Figure 2. Effect of overhang direction. (**A**) Gel electrophoresis (2% agarose gel and 1 × TBE buffer) results demonstrated the nonspecific *trans*-degradation of dsDNA substrate with 3′ overhang and 5′ overhang of the same length. In each panel, Ln1: negative control (no target); Ln2, Ln3 and Ln4: experimental lanes with target concentrations of 0.25, 25 and 250 nM, respectively. (**B**) Intensity diagram of each lane of (A). Left panel: intensity diagrams for 3′ overhang dsDNA reporter; Right panel: intensity diagrams for 5′ overhang dsDNA reporter. (**C**) Normalized lane intensities were plotted against different target concentrations for same reporters with 3′ overhang and 5′ overhang ($n = 3$ parallel experiments). Ra-3′ is derived from Ra by removing 12 nts from one end to make it 3′ overhang dsDNA; and Ra-5′ is derived from Ra by removing 12 nts from one end to make it 5′ overhang dsDNA. Cyan shade in Ra-3′ and Ra-5′ indicates the same sequence. Abbreviations: c, negative control; nM, nanomolar; bp, base pair; Ln, lane; TBE, Tris-borate EDTA; dsDNA, double-stranded DNA; nt, nucleotide; a.u., arbitrary unit.

similar degree of *trans*-degradation to Ra-5′ (Supplementary Figure S3a, Left and Middle panels), which suggests that the density or physical location (left vs. right) of the overhang does not matter. What really matters is the chemical location of the overhang (3′ versus 5′ end). Besides, we designed a 100 bp blunt-end dsDNA with a 12 nt single-strand break in the middle to resemble a new hybrid substrate with both 3′ and 5′ overhangs (Supplementary Figure S4, and sequences in Supplementary Table S1). After CRISPR reaction, we observed that the dsDNA backbone that possessed 3′ overhang got degraded preferentially (Supplementary Figure S4b, gel image), which gives an additional confirmation for Cas12a-based preferential *trans*-cleaving phenomenon.

Trans-degradation of 3′ and 5′ overhang dsDNA reporter containing the same overhang or ds backbone sequence

In the previous tests, the sequences of 3′ or 5′ overhangs are different. Here, we further studied whether the selective *trans*-cleavage is dependent on a particular overhang or backbone sequence. Supplementary Figure S5 shows a modified Ra-5′ reporter named Ra-5′s, whose overhang sequence is exactly the same as the overhang of the previous Ra-3′ reporter. We performed the CRISPR-Cas12a reaction at 25 nM and 250 nM target concentrations using reporter Ra-3′ and Ra-5′s. The gel image results in Supplementary Figure S5 show that the complete degradation was only observed for Ra-3′ but not Ra-5′s reporter, despite their similar overhang sequences. This suggests the overhang sequence did not play a significant role.

Next, we kept both sequences of the backbone and overhang the same (Ras-5′ and Ra-3′ reporters). We ran CRISPR-Cas12a assay with 25 pM, 250 pM, 2.5 nM, and 25 nM of targets, together with a negative control. From gel image results in Figure 3a, we noticed that a significant *trans*-degradation was only observed for Ra-3′ reporter (particularly for 25 and 250 nM target concentrations). For Ras-5′, only band downshifting and slight degradation were observed at higher target concentrations. To obtain quantitative results, we plotted the intensity of each lane (Figure 3b) and compared the normalized intensity values against different target concentrations in a bar chart (Figure 3C). Figure 3C shows that the normalized lane intensities for Ra-3′ reporter (green) are remarkably lower than that for Ras-5′ (blue). Despite their similar backbone and overhang sequences, the distinct *trans*-cleavage properties of Ra-3′ and Ras-5′ were further confirmed in a repeated experiment with high target concentrations (25 and 250 nM, Supplementary Figure S6). The left panel in Supplementary Figure S6 shows the complete degradation of Ra-3′ reporter with 3′ overhang, yet a lower degree of degradation was observed when we used Ras-5′ reporter with 5′ overhang. These results suggest that the overhang sequence did not affect the substrate *trans*-cleavage at all; the backbone sequence had a mild influence on the substrate *trans*-cleavage (e.g.

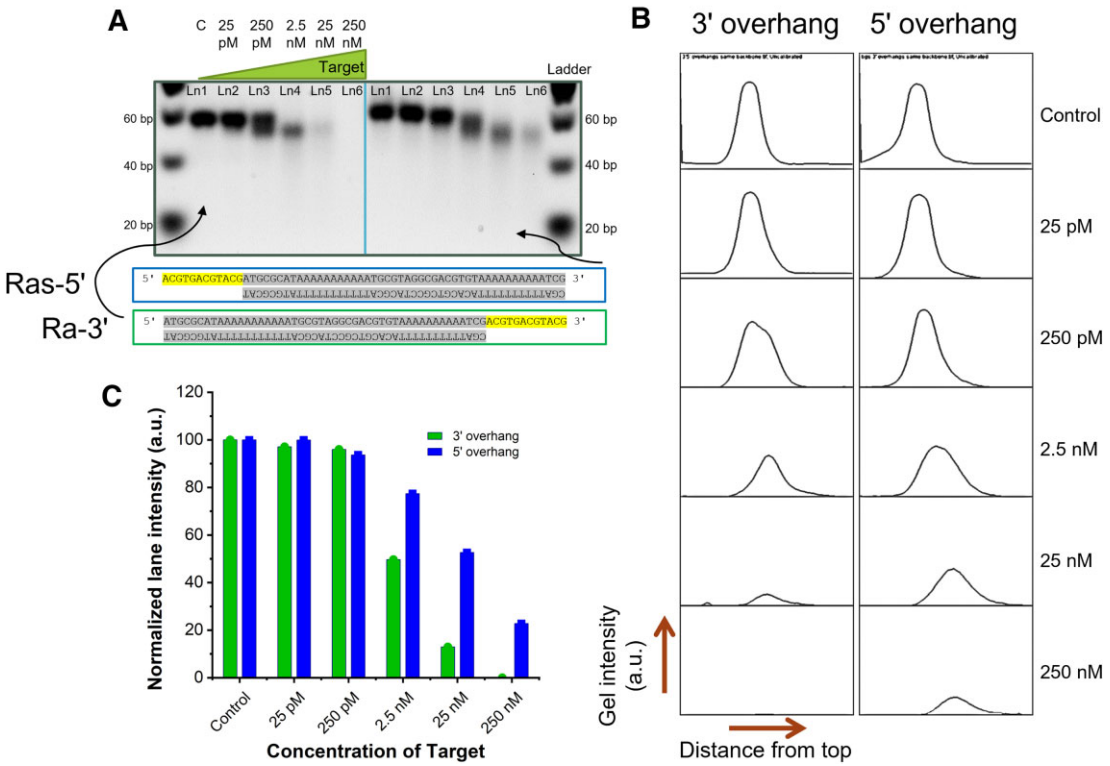

Figure 3. Effect of overhang and backbone sequences. (same ds backbone with same overhang sequence). (**A**) Gel electrophoresis (2% agarose gel and 1 × TBE buffer) results demonstrating the nonspecific *trans*-degradation of dsDNA substrate with 3′ overhang and 5′ overhang. In each panel, Ln1: negative control (no target); Ln2, Ln3, Ln4, Ln5 and Ln6: experimental lanes with target concentrations of 25 pM, 250 pM, 2.5 nM, 25 nM and 250 nM, respectively. (**B**) Intensity diagram of each lane of (A, background subtracted, not shown). Left panel: intensity diagrams for 3′ overhang dsDNA reporter (Ra-3′); Right panel: intensity diagrams for 5′ overhang dsDNA reporter (Ras-5′). (**C**) Normalized lane intensities plotted against different target concentrations for Ra-3′and Ras-5′ reporters. Ra-3′ is derived from Ra by removing 12 nts from one end to make it 3′ overhang dsDNA; and Ras-5′ has the same ds backbone and same overhang sequence as Ra-3′, but the overhang is at 5′ end. The color shade indicates the same sequence. Abbreviations: c, negative control; pM, picomolar; nM, nanomolar; bp, base pair; Ln, lane; TBE, Tris-borate EDTA; dsDNA, double-stranded DNA; nt, nucleotide; a.u., arbitrary unit.

Ra-3′ versus Rb-3′ versus Rc-3′ in Supplementary Figure S3), which requires further studies. The overhang terminal location (5′ versus 3′ end) is still the most influencing factor affecting the *trans*-cleavage property of the dsDNA reporter.

To obtain quantitative kinetic parameters, we performed another assay where we used a Qubit Flex fluorometer to measure the concentrations of dsDNA reporters in the reaction mixtures over the reaction course (up to 2 h, see the Materials and Methods section for details). We took measurements every 10–30 mins and plotted the loss of dsDNA (see details in the Materials and Methods section) against time for various substrate concentrations ([Ra-3′ or Ras-5′] = 40 to 600 nM) (Figure 4C). Then, we generated the Michaelis Menten (MM) plot by calculating the slope of time course data in Figure 4C (which was V_0) and plotted them against substrate concentrations (Figure 4D). From the MM plot, we calculated the turnover rate (K_{cat}) for Ra-3′ and Ras-5′. Our result shows that the K_{cat} value for Ra-3′ (K_{cat} = 36.4 h^{-1}) is almost 3 times of that for Ras-5′ (K_{cat} = 13.5 h^{-1}). Other kinetic parameters (e.g. K_m, V_{max}) of these two reporters are also calculated and listed in Supplementary Table S3. When we compare the turnover rate for these reporters with the conventional ssDNA F-Q reporters, we found that the turnover rate for the new overhang-containing dsDNA reporters is still slower than most ssDNA F-Q reporters (e.g. the recently reported '8C-ssDNA' F-Q reporter exhibited a K_{cat} of 0.43 s^{-1}) (Supplementary Table S4) (8,51). However, it is worth mentioning that the turnover rate of the dsDNA reporters with overhangs is heavily influenced by the size of the dsDNA backbone. By tuning the length of dsDNA backbone and ss overhang, the turnover rate of the hybrid reporters could be further optimized. Nevertheless, the higher K_{cat} value for Ra-3′ compared to Ras-5′ confirms our central hypothesis that CRISPR-Cas12a preferentially *trans*-degrades dsDNA substrates with 3′ overhang over 5′ overhang.

Hypothesized mechanism on preferable *trans*-cleavage behavior of cas12a on 3′ overhang dsDNA substrate

It is important to understand why 3′ toehold could act as a molecular key, which can turn *trans*-inactive dsDNA substrates into *trans*-active format for Cas12a. While the role of RuvC domain, which contains a catalytic pocket for

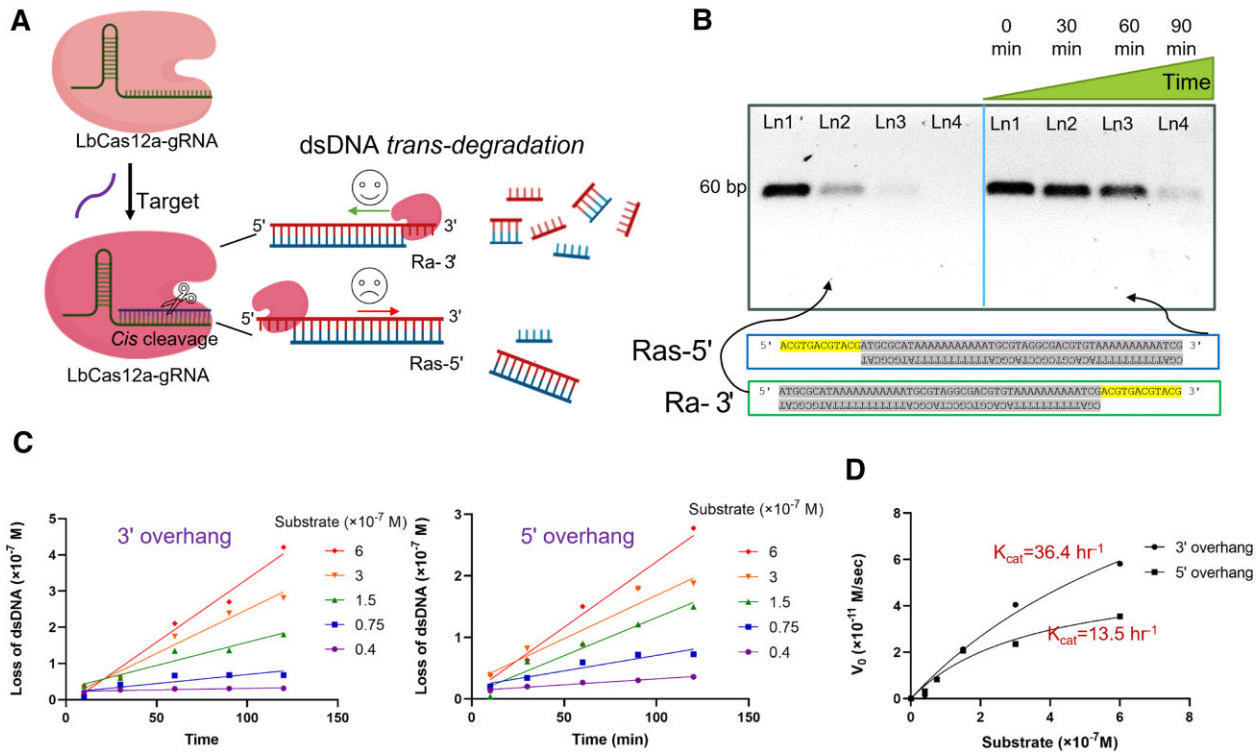

Figure 4. Reaction kinetics of hybrid reporters (same ds backbone with same overhang sequence). (**A**) Schematic showing Cas12a favorably degrades 3′ overhang dsDNA over 5′ overhang dsDNA. (**B**) Gel electrophoresis (2% agarose gel and 1 × TBE buffer) results demonstrate the nonspecific degradation of dsDNA substrate with 3′ overhang and 5′ overhang. In each panel, Ln1, Ln2, Ln3 and Ln4: CRISPR-Cas12a reaction performed for 0, 30, 60 and 90 min, respectively. For each lane, Cas12a was activated with 15 nM target concentration. (**C**) Reaction rates measurement; Left: 3′ overhang reporter (Ra-3′), Right: 5′ overhang reporter (Ras-5′). (**D**) Michaelis Menten (MM) plot. Ra-3′ is derived from Ra by removing 12 nts from one end to make it 3′ overhang dsDNA; and Ras-5′ has the same ds backbone and overhang sequence as Ra-3′, but the overhang is at 5′ end. The same color shade indicates the same sequence. Abbreviations: c, negative control; nM, nanomolar; bp, base pair; Ln, lane; TBE, Tris-borate EDTA; dsDNA, double-stranded DNA; nt, nucleotide; M, molar concentration; V_0, initial reaction velocity.

sequence-specific target cleavage in *cis*, is well understood (48), the role of Nuc domain remains to be confirmed. Some recent studies have implied that the Nuc domain plays an important role in target DNA binding (52,53), unwinding (48) and positioning of the target strand (TS), which promotes the target insertion into the RuvC catalytic site (48). However, there are not many studies on its function in the *trans* mode. Based on the experimental results, we developed the following hypotheses: (i) The Nuc domain may preferably bind ss sequences over ds sequences in the *trans* mode, which explains why an overhang can greatly promote the *trans*-cleavage activity of Cas12a against dsDNA substrates and (ii) the catalyzing effect of RuvC domain and/or unwinding of Nuc domain have directional properties, acting in a unique direction from 3′ to 5′. This contributes to the strong preference of 3′ overhang over 5′ overhang in Cas12a's *trans*-action. Together, the combined function of RuvC and Nuc domains may be responsible for the unidirectional *trans*-cleaving of Cas12a. Figure 5 depicts our hypotheses and illustrates what might be happening when Cas12a encounters two different dsDNA substrates with 3′ and 5′ overhangs, respectively. The left panel of Figure 5 shows when 3′ overhang dsDNA is present in the CRISPR reaction, the Nuc domain of *cis*-activated Cas protein first binds on the ss toehold of the dsDNA substrate, and helps unwind the nearest ds sequence. Then, the RuvC catalytic pocket starts cutting the overhang-containing strand from 3′ →5′ direction. After its quickly trimming of the ss overhang off from the dsDNA backbone, the Cas protein will continue moving into the dsDNA region and degrade the unwound ds sequences (Figure 3A). It is unclear whether the RuvC domain cuts the two strands of the dsDNA reporter simultaneously or not, but very likely it may degrade the overhang strand first and then cleaves the complementary strand also in the 3′ →5′ direction. The final result is the complete degradation of dsDNA reporter molecules, as shown in the gel results (Figure 2A, left). In contrast, when 5′ overhang dsDNA is present (Figure 5, right panel), the Nuc domain also binds on the ss toe, and the RuvC domain starts nonspecific cutting. However, due to the directional RuvC-cleaving and/or Nuc-unwinding (3′ →5′), the Cas protein only moves towards the terminal of the 5′ overhang instead of moving to the dsDNA backbone. The end result is that the Cas12a only trims the 5′ overhang, detaches it from the dsDNA backbone, but leaves the ds portion of the reporter molecules largely intact. Reflected in the gel image results, a slightly downward band with smaller molecular weight is observed in most cases (Figure 2A, right). Molecular simulation studies are ongoing to confirm these hypotheses.

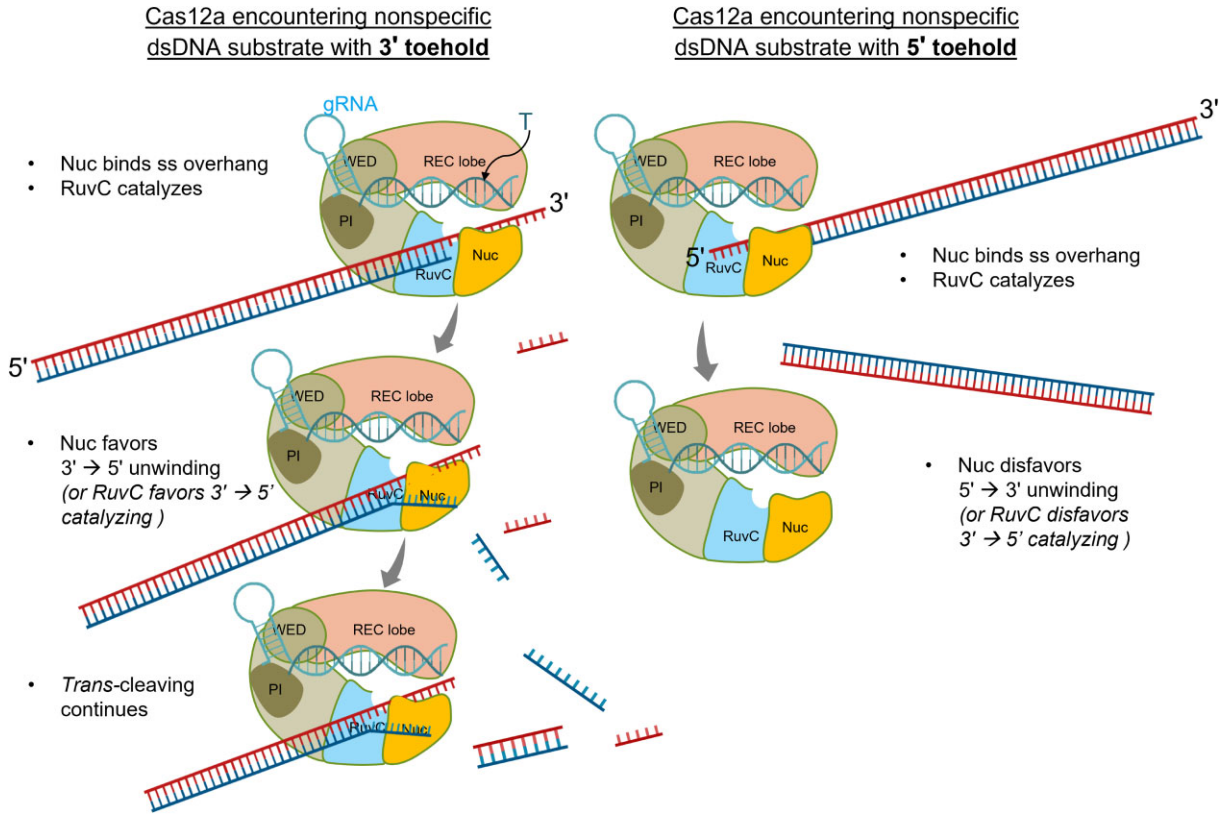

Figure 5. Hypothetical mechanism demonstrating how CRISPR-Cas12a prefers directional cleaving of hybrid reporter molecules with overhangs. Abbreviations: gRNA, guide RNA; T, ssDNA target.

Ultrasensitive CRISPR-cas12a assay based on the hybrid reporter with an overhang

To date, most of CRISPR-Dx have been developed based on the *trans*-cleavage of ssDNA substrates (8). Recently, researchers demonstrated the use of dsDNA as new reporter molecules (45,46). These dsDNA reporter molecules are typically 25–30 bp long with blunt ends and can achieve a detection sensitivity on the same order of magnitude of the ssDNA F-Q reporting platform (LOD∼10 pM, without preamplification) although at a much slower reaction rate (Supplementary Table S4)(36,45,46). Our previous work discovered that long ds λ DNA could also be used as the *trans*-cleavage substrate for Cas12a, and achieved an improved LOD down to ∼0.25 pM (12). In this work, we demonstrated that an overhang (more specifically 3′ overhang) could serve as a molecular switch, to convert relatively 'inert' dsDNA substrate into an active *trans*-reporter molecule for the CRISPR-Cas12a reaction. This new discovery could lead to a new class of reporter molecules for Cas12a-based CRISPR-Dx assays, namely the *hybrid reporter* by extending blunt-end dsDNA with a short 3′ overhang. Compared with previous ss F-Q reporters or blunt-end dsDNA reporters, the hybrid reporter combines the advantages of both types, such as low cost, high sensitivity, and reasonable reaction rate, and therefore could be a better choice for future assay development (Supplementary Table S4). We demonstrate the use of the size change (nonoptical) of the hybrid reporters for sensitive target concentration quantification in the following section, and we believe such hybrid reporters could also be fluorescently labeled and support optical readout as well.

For the hybrid reporter-based assay, we designed a reporter with a 30-bp dsDNA backbone and 12-nt 3′ overhang (Rd-3′, Figure 6). We first confirmed the directionality of the new reporter molecule. Figure 6A shows a higher *trans*-degradation rate of 3′ overhang dsDNA than that of 5′ overhang dsDNA. Then, we explored the detection sensitivity of the 3′ overhang dsDNA reporter for a wide range of target concentrations (2.5 fM to 2.5 nM). Figure 6B shows the gel results after 3 hrs of CRISPR-Cas12a reaction. The gel image results show that it is able to detect synthetic ssDNA target in a one-step CRISPR-Cas12a reaction as low as 250 fM using this hybrid reporter and naked-eye examination of the gel images. This LOD is comparable to performance of the λ DNA-based CRISPR-Cas12a assay, and superior to most ssDNA F-Q reporters or blunt-end dsDNA reporters (Supplementary Table S4). Supplementary Figure S7a shows the gel results of the repeated Rd-3′-based CRISPR-Cas12a assay for 1 h reaction time. The solid green line confirms the LOD by visible inspection, which is around 250 fM even for a much shorter reaction time. In contrast, the ssDNA counterpart reporter (the sense strand of Rd-3′) can only provide a detection limit down to 2.5 nM under the same reaction conditions (Supplementary Figure S7b). These findings suggested that hybrid reporter could greatly outperform blunt-end dsDNA or ss F-Q reporters in terms of detection sensitivity.

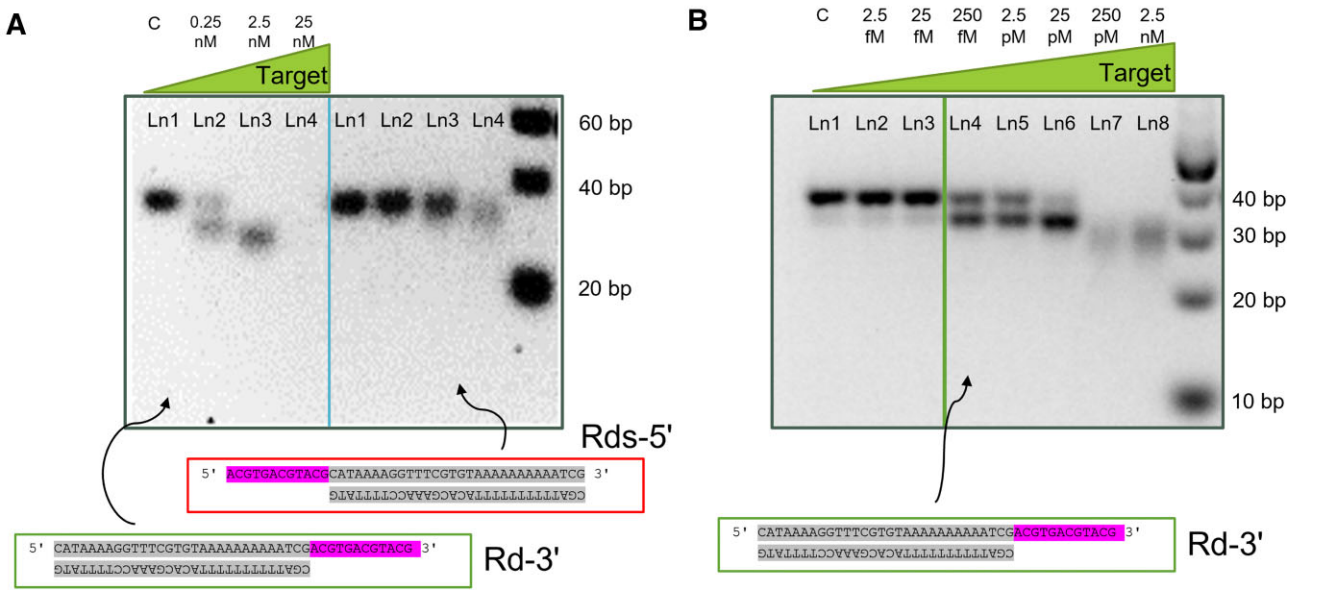

Figure 6. Ultrasensitive CRISPR-Cas12 assay based on hybrid reporters. (**A**) Gel electrophoresis (4% agarose gel and 1 × TBE buffer) results demonstrating the nonspecific *trans*-degradation of dsDNA substrate with 3′ overhang and 5′ overhang (30-bp ds backbone and 12-nt overhang sequence). In each panel in (A), Ln1: negative control (no target); Ln2, Ln3 and Ln4: experimental lanes with target concentrations of 0.25, 2.5 and 25 nM, respectively; rightmost unlabeled lane: 20 bp ladder. (**B**) Gel electrophoresis (4% agarose gel and 1 × TBE buffer) results demonstrate the detection of ssDNA targets by using hybrid reporter (ds backbone with 3′ overhang, Rd-3′) for a 3-h reaction. In (B), Ln1: negative control (no target); Ln2 to Ln8: experimental lanes with target concentrations of 2.5 fM, 25 fM, 250 fM, 2.5 pM, 25 pM, 250 pM and 2.5 nM, respectively; rightmost unlabeled lane: 10 bp ladder. Rd-3′ and Rds-5′ have the same dsDNA backbone and same overhang sequence at two different directions. The sequences in same color shade are the same. Abbreviations: c, negative control; fM, femtomolar; pM, picomolar; nM, nanomolar; bp, base pair; Ln, lane; TBE, Tris-borate EDTA; dsDNA, double-stranded DNA.

Finally, we tested the universality of the hybrid reporters for detecting various targets. First, we checked if the newly discovered CRISPR-Cas12a-based preferential *trans*-degradation is also valid for dsDNA targets. Notably, Supplementary Figure S8 demonstrates that each tested dsDNA target resulted in considerably higher degree of *trans*-cleavage for the 3′ overhang reporter than the 5′ overhang reporter. This compelling evidence affirms the directionality preference of Cas12a equally effective for dsDNA targets, thereby highlighting its immense potential for detecting a wide range of dsDNA targets. Next, we chose two real-life viral genomes: Adeno-associated viruses (AAV) and human papillomavirus 16 (HPV16), and used their genetic markers (sequences in Supplementary Table S1) as the model targets for the hybrid reporter-based CRISPR-Cas12a assay. We constructed Rd-3′ and Rds-5′ dsDNA reporters with 3′ overhang and 5′ overhang, respectively, for side-by-side comparison (sequences in Supplementary Table S1). After 1-hr reaction, the gel images in Supplementary Figure S9 show that *trans*-activated Cas12a degraded Rd-3′ at a much greater extent than Rds-5′ for both targets (results are more prominent for 2.5 and 25 nM target concentrations). We repeated this assay with very low target concentrations (25 fM to 250 pM) of AAV and HPV16 using Rd-3′ as a hybrid reporter. The results showed that our assay could detect these targets as low as 2.5 pM in an unoptimized condition (Supplementary Figure S10). It is worth noting that the best LOD could vary based on a specific target. of the LOD is also dependent on crucial parameters such as reaction temperature, gRNA sequence, and buffer composition (12,46,54). Nevertheless, these preliminary results demonstrate the feasibility of detecting real targets by using the newly developed hybrid reporters.

In summary, ssDNA reporters currently dominate the CRISPR-Dx based on the *trans*-cleavage behavior of Cas enzymes. In this work, we observed that CRISPR-Cas12a could effectively *trans*-degrade dsDNA substrates containing a 3′ overhang with a minimum length of ∼8 nt length. Such overhang-activated *trans*-cleavage is independent on the overhang or backbone sequences. More interestingly, *trans*-degradation of dsDNA substrates is not significant with a 5′ overhang sequence, but strongly prefers 3′ overhang. We attribute the notable overhang preference of Cas12a to its plausible unidirectionality in RuvC and/or Nuc domains, as well as the preferable binding properties of the Nuc domain to the ss sequences over ds sequences. The fundamental mechanism of the unidirectional *trans*-cleavage still requires a further study. We utilized the unique property of the 3′ overhang preference in dsDNA *trans*-cleavage to design a simple, low-cost, sensitive, and non-fluorescent hybrid reporter for the CRISPR-Cas12a system. The new hybrid reporter-based CRISPR-Cas12a assay detects synthetic ssDNA targets with a LOD of 250 fM by naked eye and without any preamplification steps, superior to the performance of many previous blunt-end dsDNA reporters and can enrich the CRISPR-Dx substrate library by providing a promising alternative to conventional ssDNA F-Q reporters. Our study not only unveils a new interesting biological behavior of Cas12a protein, but only provides options for developing ultrasensitive biosensing platform using a new class of hybrid DNA reporter molecules.

DATA AVAILABILITY

The data underlying this article are available in the article and in its online supplementary material.

SUPPLEMENTARY DATA

Supplementary Data are available at NAR Online.

FUNDING

National Science Foundation [1944167]. Funding for open access charge: Federal funding.
Conflict of interest statement. None declared.

REFERENCES

1. Jinek,M., Chylinski,K., Fonfara,I., Hauer,M., Doudna,J.A. and Charpentier,E. (2012) A programmable dual-RNA–guided DNA endonuclease in adaptive bacterial immunity. *Science*, **337**, 816–821.
2. Horvath,P. and Barrangou,R. (2010) CRISPR/Cas, the immune system of bacteria and archaea. *Science*, **327**, 167–170.
3. Wiedenheft,B., Sternberg,S.H. and Doudna,J.A. (2012) RNA-guided genetic silencing systems in bacteria and archaea. *Nature*, **482**, 331–338.
4. Cong,L., Ran,F.A., Cox,D., Lin,S., Barretto,R., Habib,N., Hsu,P.D., Wu,X., Jiang,W. and Marraffini,L.A. (2013) Multiplex genome engineering using CRISPR/Cas systems. *Science*, **339**, 819–823.
5. Ledford,H. and Callaway,E. (2020) Pioneers of revolutionary CRISPR gene editing win chemistry Nobel. *Nature*, **586**, 346–347.
6. Kim,J. and Kim,J.-S. (2016) Bypassing GMO regulations with CRISPR gene editing. *Nat. Biotechnol.*, **34**, 1014–1015.
7. Cyranoski,D. (2016) CRISPR gene-editing tested in a person for the first time. *Nature*, **539**, 479.
8. Chen,J.S., Ma,E., Harrington,L.B., Da Costa,M., Tian,X., Palefsky,J.M. and Doudna,J.A. (2018) CRISPR-Cas12a target binding unleashes indiscriminate single-stranded DNase activity. *Science*, **360**, 436–439.
9. Gootenberg,J.S., Abudayyeh,O.O., Lee,J.W., Essletzbichler,P., Dy,A.J., Joung,J., Verdine,V., Donghia,N., Daringer,N.M., Freije,C.A. *et al.* (2017) Nucleic acid detection with CRISPR-Cas13a/C2c2. *Science (New York, N.Y.)*, **356**, 438–442.
10. Kaminski,M.M., Abudayyeh,O.O., Gootenberg,J.S., Zhang,F. and Collins,J.J. (2021) CRISPR-based diagnostics. *Nat. Biomed. Eng.*, **5**, 643–656.
11. Weng,Z., You,Z., Yang,J., Mohammad,N., Lin,M., Wei,Q., Gao,X. and Zhang,Y. (2023) CRISPR-Cas biochemistry and CRISPR-based molecular diagnostics. *Angew. Chem. Int. Ed.*, **62**, e202214987.
12. Mohammad,N., Katkam,S.S. and Wei,Q. (2022) A sensitive and nonoptical CRISPR detection mechanism by sizing double-stranded λ DNA reporter. *Angew. Chem. Int. Ed.*, **61**, e202213920.
13. Jolany vangah,S., Katalani,C., Boone,H.A., Hajizade,A., Sijercic,A. and Ahmadian,G. (2020) CRISPR-based diagnosis of infectious and noninfectious diseases. *Biol. Proced. Online*, **22**, 22.
14. Mohammad,N., Katkam,S.S. and Wei,Q. (2022) Recent advances in CRISPR-based biosensors for point-of-care pathogen detection. *CRISPR J.*, **5**, 500–516.
15. Jiao,J., Kong,K., Han,J., Song,S., Bai,T., Song,C., Wang,M., Yan,Z., Zhang,H., Zhang,R. *et al.* (2021) Field detection of multiple RNA viruses/viroids in apple using a CRISPR/Cas12a-based visual assay. *Plant Biotechnol. J.*, **19**, 394–405.
16. Li,Y., Mansour,H., Wang,T., Poojari,S. and Li,F. (2019) Naked-eye detection of grapevine red-blotch viral infection using a plasmonic CRISPR Cas12a assay. *Anal. Chem.*, **91**, 11510–11513.
17. Hu,M., Yuan,C., Tian,T., Wang,X., Sun,J., Xiong,E. and Zhou,X. (2020) Single-step, salt-aging-free, and thiol-free freezing construction of AuNP-based bioprobes for advancing CRISPR-based diagnostics. *JACS*, **142**, 7506–7513.
18. Yuan,C., Tian,T., Sun,J., Hu,M., Wang,X., Xiong,E., Cheng,M., Bao,Y., Lin,W., Jiang,J. *et al.* (2020) Universal and naked-eye gene detection platform based on the clustered regularly interspaced short palindromic repeats/Cas12a/13a system. *Anal. Chem.*, **92**, 4029–4037.
19. Barnes,K.G., Lachenauer,A.E., Nitido,A., Siddiqui,S., Gross,R., Beitzel,B., Siddle,K.J., Freije,C.A., Dighero-Kemp,B., Mehta,S.B. *et al.* (2020) Deployable CRISPR-Cas13a diagnostic tools to detect and report Ebola and Lassa virus cases in real-time. *Nat. Commun.*, **11**, 4131–4131.
20. Ding,X., Yin,K., Li,Z., Lalla,R.V., Ballesteros,E., Sfeir,M.M. and Liu,C. (2020) Ultrasensitive and visual detection of SARS-CoV-2 using all-in-one dual CRISPR-Cas12a assay. *Nat. Commun.*, **11**, 4711–4711.
21. Fozouni,P., Son,S., Díaz de León Derby,M., Knott,G.J., Gray,C.N., D'Ambrosio,M.V., Zhao,C., Switz,N.A., Kumar,G.R., Stephens,S.I. *et al.* (2021) Amplification-free detection of SARS-CoV-2 with CRISPR-Cas13a and mobile phone microscopy. *Cell*, **184**, 323–333.
22. Nguyen,L.T., Smith,B.M. and Jain,P.K. (2020) Enhancement of trans-cleavage activity of Cas12a with engineered crRNA enables amplified nucleic acid detection. *Nat. Commun.*, **11**, 4906–4906.
23. Dai,Y., Somoza,R.A., Wang,L., Welter,J.F., Li,Y., Caplan,A.I. and Liu,C.C. (2019) Exploring the trans-cleavage activity of CRISPR-Cas12a (cpf1) for the development of a universal electrochemical biosensor. *Angew. Chem. Int. Ed.*, **58**, 17399–17405.
24. Xu,W., Jin,T., Dai,Y. and Liu,C.C. (2020) Surpassing the detection limit and accuracy of the electrochemical DNA sensor through the application of CRISPR Cas systems. *Biosens. Bioelectron.*, **155**, 112100.
25. Shi,K., Xie,S., Tian,R., Wang,S., Lu,Q., Gao,D., Lei,C., Zhu,H. and Nie,Z. (2021) A CRISPR-Cas autocatalysis-driven feedback amplification network for supersensitive DNA diagnostics. *Sci. Adv.*, **7**, eabc7802.
26. Liu,T.Y., Knott,G.J., Smock,D.C.J., Desmarais,J.J., Son,S., Bhuiya,A., Jakhanwal,S., Prywes,N., Agrawal,S., Díaz de León Derby,M. *et al.* (2021) Accelerated RNA detection using tandem CRISPR nucleases. *Nat. Chem. Biol.*, **17**, 982–988.
27. Myhrvold,C., Freije,C.A., Gootenberg,J.S., Abudayyeh,O.O., Metsky,H.C., Durbin,A.F., Kellner,M.J., Tan,A.L., Paul,L.M., Parham,L.A. *et al.* (2018) Field-deployable viral diagnostics using CRISPR-Cas13. *Science (New York, N.Y.)*, **360**, 444–448.
28. Arizti-Sanz,J., Freije,C.A., Stanton,A.C., Petros,B.A., Boehm,C.K., Siddiqui,S., Shaw,B.M., Adams,G., Kosoko-Thoroddsen,T.-S.F., Kemball,M.E. *et al.* (2020) Streamlined inactivation, amplification, and Cas13-based detection of SARS-CoV-2. *Nat. Commun.*, **11**, 5921.
29. Arizti-Sanz,J., Bradley,A.D., Zhang,Y.B., Boehm,C.K., Freije,C.A., Grunberg,M.E., Kosoko-Thoroddsen,T.-S.F., Welch,N.L., Pillai,P.P., Mantena,S. *et al.* (2022) SimplifiedCas13-based assays for the fast identification of SARS-CoV-2 and its variants. *Nat. Biomed. Eng.*, **6**, 932–943.
30. Patchsung,M., Jantarug,K., Pattama,A., Aphicho,K., Suraritdechachai,S., Meesawat,P., Sappakhaw,K., Leelahakorn,N., Ruenkam,T., Wongsatit,T. *et al.* (2020) Clinical validation of a Cas13-based assay for the detection of SARS-CoV-2 RNA. *Nat. Biomed. Eng.*, **4**, 1140–1149.
31. Wang,X., Ji,P., Fan,H., Dang,L., Wan,W., Liu,S., Li,Y., Yu,W., Li,X., Ma,X. *et al.* (2020) CRISPR/Cas12a technology combined with immunochromatographic strips for portable detection of African swine fever virus. *Commun. Biol.*, **3**, 62–62.
32. Mukama,O., Yuan,T., He,Z., Li,Z., Habimana,J.d.D., Hussain,M., Li,W., Yi,Z., Liang,Q. and Zeng,L. (2020) A high fidelity CRISPR/Cas12a based lateral flow biosensor for the detection of HPV16 and HPV18. *Sens. Actuators B: Chem.*, **316**, 128119.
33. Ding,X., Yin,K., Li,Z., Sfeir,M.M. and Liu,C. (2021) Sensitive quantitative detection of SARS-CoV-2 in clinical samples using digital warm-start CRISPR assay. *Biosens. Bioelectron.*, **184**, 113218–113218.
34. Park,J.S., Hsieh,K., Chen,L., Kaushik,A., Trick,A.Y. and Wang,T.-H. (2021) Digital CRISPR/Cas-Assisted Assay for Rapid and Sensitive Detection of SARS-CoV-2. *Adv. Sci.*, **8**, 2003564–2003564.
35. Wu,X., Tay,J.K., Goh,C.K., Chan,C., Lee,Y.H., Springs,S.L., Wang,D.Y., Loh,K.S., Lu,T.K. and Yu,H. (2021) Digital CRISPR-based method for the rapid detection and absolute quantification of nucleic acids. *Biomaterials*, **274**, 120876.
36. Yu,T., Zhang,S., Matei,R., Marx,W., Beisel,C.L. and Wei,Q. (2021) Coupling smartphone and CRISPR–Cas12a for digital and multiplexed nucleic acid detection. *AIChE J.*, **67**, e17365.
37. Gootenberg,J.S., Abudayyeh,O.O., Kellner,M.J., Joung,J., Collins,J.J. and Zhang,F. (2018) Multiplexed and portable nucleic acid detection

platform with Cas13, Cas12a, and Csm6. *Science (New York, N.Y.)*, **360**, 439–444.
38. Ackerman,C.M., Myhrvold,C., Thakku,S.G., Freije,C.A., Metsky,H.C., Yang,D.K., Ye,S.H., Boehm,C.K., Kosoko-Thoroddsen,T.-S.F., Kehe,J. *et al.* (2020) Massively multiplexed nucleic acid detection with Cas13. *Nature*, **582**, 277–282.
39. Welch,N.L., Zhu,M., Hau,C., Weller,J., Mirhashemi,M.E., Mantena,S., Nguyen,T.G., Shaw,B., Ackerman,C.M. and Thakku,S.G.J.m. (2021) Multiplexed CRISPR-based microfluidic platform for clinical testing of respiratory viruses and SARS-CoV-2 variants. *Nat. Med.*, **28**, 1083–1094.
40. Ali,Z., Aman,R., Mahas,A., Rao,G.S., Tehseen,M., Marsic,T., Salunke,R., Subudhi,A.K., Hala,S.M., Hamdan,S.M. *et al.* (2020) iSCAN: an RT-LAMP-coupled CRISPR-Cas12 module for rapid, sensitive detection of SARS-CoV-2. *Virus Res.*, **288**, 198129–198129.
41. Bai,J., Lin,H., Li,H., Zhou,Y., Liu,J., Zhong,G., Wu,L., Jiang,W., Du,H., Yang,J. *et al.* (2019) Cas12a-based on-site and rapid nucleic acid detection of African swine fever. *Front. Microbiol.*, **10**, 2830–2830.
42. Chaijarasphong,T., Thammachai,T., Itsathitphaisarn,O., Sritunyalucksana,K. and Suebsing,R. (2019) Potential application of CRISPR-Cas12a fluorescence assay coupled with rapid nucleic acid amplification for detection of white spot syndrome virus in shrimp. *Aquaculture*, **512**, 734340.
43. Pang,Y., Li,Q., Wang,C., zhen,S., Sun,Z. and Xiao,R. (2022) CRISPR-cas12a mediated SERS lateral flow assay for amplification-free detection of double-stranded DNA and single-base mutation. *Chem. Eng. J.*, **429**, 132109.
44. Li,S.-Y., Cheng,Q.-X., Liu,J.-K., Nie,X.-Q., Zhao,G.-P. and Wang,J. (2018) CRISPR-Cas12a has both cis-and trans-cleavage activities on single-stranded DNA. *Cell Res.*, **28**, 491.
45. Smith,C.W., Nandu,N., Kachwala,M.J., Chen,Y.-S., Uyar,T.B. and Yigit,M.V. (2020) Probing CRISPR-Cas12a nuclease activity using double-stranded DNA-templated Fluorescent Substrates. *Biochem.*, **59**, 1474–1481.
46. Smith,C.W., Kachwala,M.J., Nandu,N. and Yigit,M.V. (2021) Recognition of DNA target formulations by CRISPR-Cas12a using a dsDNA reporter. *ACS Synth. Biol.*, **10**, 1785–1791.
47. Fuchs,R.T., Curcuru,J., Mabuchi,M., Yourik,P. and Robb,G.B. (2019) Cas12a trans-cleavage can be modulated in vitro and is active on ssDNA, dsDNA, and RNA. bioRxiv doi: https://doi.org/10.1101/600890, 08 April 2019, preprint: not peer reviewed.
48. Swarts,D.C. and Jinek,M. (2019) Mechanistic insights into the cis-and trans-acting DNase activities of Cas12a. *Mol. Cell*, **73**, 589–600.
49. Lee,S., Nam,D., Park,J.S., Kim,S., Lee,E.S., Cha,B.S. and Park,K.S. (2022) Highly efficient DNA reporter for CRISPR/Cas12a-based specific and sensitive biosensor. *Biochip J.*, **16**, 463–470.
50. Murugan,K., Seetharam,A.S., Severin,A.J. and Sashital,D.G. (2020) CRISPR-Cas12a has widespread off-target and dsDNA-nicking effects. *JBC*, **295**, 5538–5553.
51. Lv,H., Wang,J., Zhang,J., Chen,Y., Yin,L., Jin,D., Gu,D., Zhao,H., Xu,Y. and Wang,J. (2021) Definition of CRISPR Cas12a trans-cleavage units to facilitate CRISPR diagnostics. *Front. Microbiol.*, **12**, 766464.
52. Swarts,D.C., van der Oost,J. and Jinek,M. (2017) Structural basis for guide RNA processing and seed-dependent DNA targeting by CRISPR-Cas12a. *Mol. Cell*, **66**, 221–233.
53. Stella,S., Mesa,P., Thomsen,J., Paul,B., Alcón,P., Jensen,S.B., Saligram,B., Moses,M.E., Hatzakis,N.S. and Montoya,G. (2018) Conformational activation promotes CRISPR-Cas12a catalysis and resetting of the endonuclease activity. *Cell*, **175**, 1856–1871.
54. Nouri,R., Jiang,Y., Politza,A.J., Liu,T., Greene,W.H., Zhu,Y., Nunez,J.J., Lian,X. and Guan,W. (2023) STAMP-Based Digital CRISPR-Cas13a for Amplification-Free Quantification of HIV-1 Plasma Viral Loads. *ACS Nano*, **17**, 10701–10712.